HHS Public Access

Author manuscript

Mol Cancer Res. Author manuscript; available in PMC 2017 January 01.

Published in final edited form as:

Mol Cancer Res. 2016 January ; 14(1): 66–77. doi:10.1158/1541-7786.MCR-15-0159.

p53 Deletion or Hot-spot Mutations Enhance mTORC1 Activity by Altering Lysosomal Dynamics of TSC2 and Rheb

Stuti Agarwal[1,*], **Catherine M. Bell**[1,*], **Shirley M. Taylor**[2], and **Richard G. Moran**[1]

[1]Department of Pharmacology & Toxicology, Virginia Commonwealth University, Richmond, VA 23298

[2]Department of Microbiology & Immunology and Massey Cancer Center, Virginia Commonwealth University, Richmond, VA 23298

Abstract

The activity of mammalian target of rapamycin complex 1 (mTORC1) is frequently enhanced in carcinomas, an effect thought to contribute to the malignant phenotype. Here, it is demonstrated that either deletion or mutation of TP53 in colon or lung carcinoma cells substantially enhances mTORC1 kinase activity by an effect downstream of and independent of AMPK. Mechanistically, it was determined that loss or mutation of p53 decreased expression of TSC2 and Sestrin2 (SESN2). Complementation of p53 null cells with TSC2 or Sestrin2 reduced mTORC1 activity to levels found in p53 wt cells, while their genetic depletion enhanced mTORC1 activity in p53 wt cells. However, the primary causal event in enhanced mTORC1 activity upon loss of p53 appeared to be a diminished distribution of TSC2 to lysosomal membranes containing mTOR. Subsequently, there was increased Rheb in the lysosomal compartment, and a higher mTOR association with Raptor. Transfection of TSC2 into p53 null cells replaced TSC2 and diminished Rheb at the lysosome, recapitulating cells with wt p53. In contrast, transfection of Sestrin2 decreased mTOR in lysosomes, but the lower levels of Sestrin2 in p53 null cells did not change lysosomal mTOR. In summary, loss of the transcriptional activity of p53, either by deletion or by key mutations in the DNA-binding domain, diminishes expression of TSC2 and Sestrin2, thus, shifting membrane-bound TSC2 out of lysosomal membranes, increasing lysosomal Rheb and increasing the kinase activity of mTORC1.

Implications—This study establishes that loss of p53 function decreases lysosomal TSC2 and increases lysosomal Rheb resulting in hyperactive mTORC1, findings that are consistent with a more malignant phenotype.

Graphical Abstract

Corresponding Author: Richard G. Moran, Massey Cancer Center, 401 College Street, Richmond, VA 23298-0035. Tel: 804-828-5783, rmoran@vcu.edu.

*These authors contributed equally to this work.

Conflict of Interest. The authors disclose no conflicts of interest.

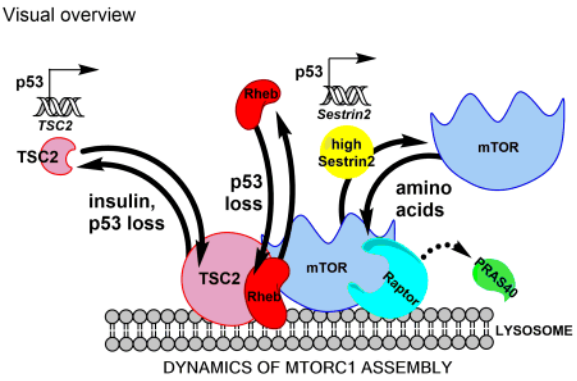

Keywords

mTOR; mutant p53; TSC2; Rheb; lysosomal membranes

The mammalian target of rapamycin (mTOR) is a highly conserved regulator of cell growth and proliferation in eukaryotes. mTOR is present as two functionally distinct complexes: mTORC1, which has kinase activity towards two proteins rate-limiting to cap-dependent protein synthesis initiation, 4EBP1 and p70-S6K1 (S6K1), and mTORC2, that phosphorylates Akt at S473 (1–3). The mTORC1 complex includes the catalytic subunit mTOR, PRAS40, an mTOR inhibitor inactivated by phosphorylation by Akt at T246, and Raptor, which acts as a scaffold for the recruitment of the substrates 4EBP1 and S6K1 (4). mTORC1 activity is localized on a subcellular membrane compartment (5) recently determined to be lysosomal membranes (6), which acts as the assembly site of the several components of this complex. This subcellular organization is critical for the regulation of mTORC1 activity: the activation of mTORC1 by amino acids involves the partitioning of mTOR onto lysosomes (7–11) and stimulation of mTORC1 by insulin involves induction of the dissociation of tuberin (TSC2) from proximity to mTOR on lysosomal membranes (5,6). TSC2 facilitates the conversion of the obligatory mTORC1-activator Rheb-GTP to the inactive Rheb-GDP (12–14). Whereas the TSC1 and TBC1D7 components of the Tuberous Sclerosis Complex (TSC) appear fixed at the lysosomes, TSC2 dynamically partitions onto and off these membranes, and it is this partitioning that is currently thought to be involved in the effect of TSC2 on the ability of Rheb to activate mTORC1 (6). The Sestrin proteins have been shown to inhibit mTORC1 kinase activity and they, likewise, suppress the translocation of mTOR to the lysosome (7, 15–17).

Akt and, thereby, the downstream mTORC1 are frequently activated in human carcinomas due to mutation of upstream K-Ras and PI3K that impact control of this pathway. However, p53 is the most commonly mutated or lost gene in many tumor types, including colon and lung carcinomas; we sought to clarify the effect of p53 loss or mutation on control of mTORC1. Both TSC2 and the Sestrins have been shown to be targets for p53-directed transcription (18–20). It has been reported that the p53 response to DNA damaging agents diminishes mTORC1 activity in carcinoma cells; this effect requires the intermediate activation of the AMP-dependent protein kinase (AMPK) (21). We now report that both loss of p53 or mutation of key residues in the DNA binding domain of this tumor suppressor also

substantially upregulate mTORC1 activity by an effect that is downstream from AMPK and therefore separate from the effect of DNA-damage stabilized p53. The lower levels of TSC2 in p53 null or mutant cells were causally linked to the activation of mTORC1, apparently by increasing the association of Rheb with lysosomal membranes thereby increasing active mTORC1 complexes.

Materials and Methods

Cell culture and reagents

HCT116 cell lines were a gift from Dr Bert Vogelstein. H460 and A549 cell lines were purchased from ATCC (Manassas, VA, USA.) and grown in RPMI 1640 with 10% dialyzed fetal bovine serum (dFBS). H1299 cells expressing a ponasterone-inducible p53 gene (22) were supplied by Drs. Jennifer Pietenpol and Sumitra Deb. Immortalized p53−/− TSC2−/− MEFs and Sestrin2 −/− MEFs (kind gifts of Dr. Andrei Budanov) were grown in DMEM supplemented with 10% dFBS. A549 and H460 cells were purchased from ATCC. All cell lines were frozen upon receipt and genetically modified cells were phenotypically verified as part of these experiments. Experiments were performed in dFBS. Etoposide was dissolved in dimethyl sulfoxide (DMSO). All other reagents were from Sigma Aldrich (St. Louis, MO, USA.).

Immunoblotting

Total cellular protein was extracted and immunoblotted, using 20 μg of protein as described (22,23). Antibodies from Cell Signaling Technology (Danvers, Massachusetts, USA) are; p70 S6K (Cat # 9202S), P-T389 S6K1 (Cat# 9205S), 4EBP1 (Cat# 9644P), P-T70 4EBP1 (Cat# 9455S), P-T37/46 4EBP1 (Cat# 2855L), eIF4E (Cat# 2067S), AMPK (Cat# 2793S), P-T172 AMPK (Cat# 2531S), mTOR (Cat# 2983S), P-2448 mTOR (Cat# 2971S), Raptor (Cat# 2280S), P-S792 Raptor (Cat# 2083S), TSC2 (Cat# 3990S), P-S1387 TSC2 (Cat# 5584S), PRAS40 (Cat# 2610S), P-T246 PRAS40 (Cat# 2640S), and β-Actin (Cat# 3700P). p53 antibody (Cat# OP43) is from Calbiochem (EMD, Darmstadt, Germany). Sestrin2 antibody was (Cat# 10795-1-AP) from Proteintech Group Inc. (Chicago, USA). Chemiluminescence was detected using SuperSignal Substrate (Thermo Scientific, Rockford, IL, USA.).

Immunoprecipitations

HCT116 cells were planted at 2×10^6/150 mm dish and allowed to adhere for 48 hours. Cells were harvested, lysed in 50 mM Tris-HCl, pH 7.5, 100 mM NaCl, 0.3 % CHAPS, 1 mM EDTA, 10 mM β-glycerophosphate and 1 mM Na_3VO_4 supplemented with 1x Complete Protease Inhibitor Mixture (Roche Applied Sciences). One mg of protein from the supernatants from a 15,000 xg 20 min. centrifugation was used for immunoprecipitations using either Raptor antibody or IgG and protein A- or G-Sepaharose 4FF beads (Amersham Biosciences). The IPs were washed three times with lysis buffer. For detection of Rheb, blots were incubated with anti-Rheb antibody overnight at 4 degrees with or without 1 μg (in 1 ml buffer) of the peptide used as immunogen to raise the Rheb antibody (Abcam human Rheb peptide, cat no ab194764).

Transfections and RNA interference

DharmaFECT transfection reagent no. 2, siGENOME SMARTpool siRNAs targeting human p53 and scrambled siRNA pool no. 1 were purchased from Dharmacon (GE Healthcare, Lafayette, CO, USA.). Cells were transfected with 50 nM siRNA in 0.1% DharmaFECT for 48 hrs. Protein was harvested after 48 hr. Sestrin2 +/+ and −/− MEFs were harvested and lysed 48 hrs after plating at < 50 % confluence. Lysates were assessed for levels of Sestrin2, p-T389 S6K, p-T70 4EBP1, S6K1, 4EBP1, and actin by immunoblotting. p53+/+ HCT116 cells were plated and were allowed to grow for 24 hrs, then were transfected with a pool of four siRNAs against TSC2 from Qiagen for 72 hrs as described in the Dharmafect protocol. Cells were lysed and assessed for TSC2 and p-T389 S6K1.

Generating p53 mutant stable cell lines

HCT116 p53−/− or H1299 cells were plated in 6 well plates at a density of 2×10^5 cells per well and transfection was performed 24 hrs later with 2 μg of various mutant p53 plasmids. Forty-eight hrs after transfection, cells were replated at low density, exposed to 100 μg/ml (HCT116) or 40 μg/ml (H1299) zeocin for 2 weeks and independent colonies were isolated and mass cultured.

m^7GTP capture of 4EBP1-eIF4E complexes

Cells were lysed on ice for 30 minutes in IP buffer [25 mM HEPES (pH 7.5), 1% NP40, 100 mM NaCl, 1 mM EDTA, 1 mM EGTA, 50 mM NaF, 1 mM phenylmethylsulfonylfluoride, 0.1% 2-mercaptoethanol, and Roche Complete Protease Inhibitors (Roche, Indianapolis, IN, USA.)]. 4EBP1-eIF4E complexes were captured on m^7GTP sepharose 4B beads (Cat #2705025-01, GE healthcare life sciences, Pittsburg, USA), as described previously (25). Samples were resolved on a 12.5% SDS-PAGE gel.

Kinase Assays

Recombinant human 4EBP1 (cat# SRP0253) and Rheb (cat# SRP0225) were purchased from Sigma Aldrich. GTPγS was purchased from Millipore (Billerica, MA, USA.). HCT116 cells were plated at 2×10^6 cells/15 mm dish. After 48 hr, cells were harvested and lysed with IP buffer and anti-Raptor immunoprecipitations were performed with 1 mg protein under low salt conditions (buffer with 100mM NaCl) (26). *In vitro* kinase assays were performed on immunoprecipitates (26), using recombinant 4EBP1 as substrate. Anti-Raptor antibody (Cat# 05-1470) used for IP was from Millipore.

qRT-PCR

Total RNA was isolated using TRIzol (Invitrogen/Life Tech., Grand Island, NY, USA). DNase treatment and cDNA synthesis followed the manufacturer's protocol. Real time PCRs were as described (27). Primer sequences are as follows; TSC2: 5′-TCGTGTTCCTGCAGCTCTACCATT-3′ (sense) and 5′-ACCGCTCAAAGGACTGTGACTCAT-3′, Sestrin2: 5′-ACAAGTGTTGTGGCCTT CCTGAAC-3′ (sense) and 5′-ATGGGTGAATGGCAAGTAGGAGGT-3′ (antisense), Rheb: 5′-GGCTGGGTTACAGCTGATTG-3′ (sense) and 5′-CTGACACGGACATCGAGCTA-3′ (antisense), β-actin: 5′-

CACGAAACTACCTTCAACTCC-3′ (sense) and 5′-TCATACTCCTGCTTG CTGATCC-3′ (antisense). Values were normalized to expression of β-actin.

Subcellular Fractionation

Cells from two near-confluent 15 cm dishes were washed and scraped into cold PBS with 1X protease inhibitors. Separation of total cellular membranes from cytosolic fractions was performed following the conditions in reference 5, with a final centrifugation step of 100,000 × g for 1 hr to separate out the soluble cytosolic fraction from the membrane pellet. Separation of heavy and light membrane fractions/cytosols followed the procedure in reference 6 with the final centrifugation at 20,000 × g for 2h. Protein concentrations for each fraction were normalized separately, and samples were processed for SDS-PAGE gels and immunoblotting as described (23, 24); membrane fractions were not boiled. Antibodies for subcellular fractionation analysis included: TSC2 rabbit mAB (CST, 3990), Rheb rabbit mAB (Abcam, 92313, Cambridge, MA, USA.), LDHA rabbit pAB (CST, 2012), LAMP1 rabbit mAB (CST, 9091), Integrin β1 rabbit mAB (CST, 9699), mTOR rabbit mAB (CST, 2983), Raptor rabbit mAB (CST, 2880), and PRAS40 rabbit pAB (CST, 2610).

Immunofluorescence microscopy

Cells were prepared for immunofluorescence as described (6). Primary antibodies used for immunofluorescence were validated previously (6). They included rabbit anti-TSC2 (CST, 4308, 1:800), mouse anti-Rheb (Abnova, H00006009-M01, 1:1000, Walnut, CA, USA.), rabbit anti-mTOR (CST, 2983, 1:400), rabbit anti-LAMP1 (CST, 9091, 1:200), and mouse anti-LAMP2 (Santa Cruz, 18822, 1:100, Dallas, TX, USA.). p53 knockdown studies used mouse anti-p53 (Calbiochem, OP43, 1:100). Sestrin2 was probed with rabbit anti-Sestrin2 (Proteintech group, 10795-1-AP, 1:100). Secondary antibodies for immunofluorescence were anti-rabbit Alexa Fluor 488 (Life Tech., A21206), and anti-mouse Alexa Fluor 568 (Life Technologies, A11004). Coverslips were mounted (Fisher, 12-549-3) in VECTASHIELD mounting medium with DAPI (Vector laboratories, H-1200, Burlingame, CA, USA.). Confocal images were acquired with a Zeiss LSM 700, Axio Imager 2 microscope (Zeiss, Thornwood, NY), through a 63X oil immersion objective, using sequential scanning to capture each channel. Representative cell images reflect identical detector and display settings. Optical slice thickness was set to 0.7 μm (1 Airy unit, pinhole size green = 41.07 μM, red = 43.43 μM), pixel depth 16-bit, scan speed 6, and line averaging 4. The images were 1368 × 1368 pixels (scaled = 101.61 × 101.61 μm) with a pixel size of 0.7 × 0.7 μm. Quantitative analyses were done using the colocalization function of the Zeiss Zen 2014 software. Intensity thresholds were set using single color controls for each antibody. Manders' colocalization coefficient was reported as percent colocalization (28), using 50 to 80 cells, representing five separate fields for each condition.

Overexpression of HA-TSC2 and Flag-Sestrin2

HCT116 p53 null cells were transfected with 3 μg DNA using Polyjet (DNA:Polyjet at 1:3). Cells were lysed and immunoblotted 48 hr after transfection (23,24). For m^7GTP pulldowns, cells were plated in 10 cm dishes and transfected using 3 μg DNA; 48 hr later, cells were lysed in m^7GTP buffer. 4EBP1-eIF4E complexes were captured on m^7GTP beads, as described (25). Samples were resolved on 12.5% SDS-PAGE gels. Flag-Sestrin2 plasmid

was obtained from Dr. Andrei Budanov and HA-TSC2 was purchased from Addgene (Plasmid 24939, deposited by Dr Kunliang Guan (29)).

Statistics

RT-qPCR data are expressed as ±sd, and fractionation and colocalization data as ±SEM. Significance was determined using unpaired two-tailed Student's t-tests, assuming equal variance.

Results

mTORC1 activity is substantially enhanced by loss of basal p53 function

Feng et al (21) established a connection between p53 and mTORC1 when they showed that stabilization of p53 by the DNA damaging agent VP16 (etoposide) suppressed the phosphorylation of the mTORC1 target S6K1 in MEFs and that this effect does not occur in MEFs lacking p53. We observed the same phenomena for HCT116 colon carcinoma cells isogenic for p53 deletion: the mTORC1 substrate S6K1 becomes hypophosphorylated in wild type (wt) HCT116 cells treated with VP16 but not in the isogenic p53−/− HCT116 cell line treated with VP16 (Fig. 1A). However, a second very significant effect was evident from these experiments: untreated p53−/− HCT116 cells displayed a robust hyperphosphorylation of S6K1 at T389 over that in HCT116 with wt p53 (Fig 1A, lanes 1 and 3). The effect of DNA damage on mTORC1 activity was shown by Feng et al. to involve AMPK activation; however, the stimulation of mTORC1 with loss of p53 in untreated cells was not due to differences in the activation of AMPK, as the phosphorylation of AMPK at S172 was independent of p53 (Fig. 1B). An increase in the level of 4EBP1 phosphorylated at T70, a direct measure of mTORC1 activity, was apparent in p53−/− cells compared with that in p53 wt cells (Fig. 1C). There was also a substantial decrease in the 4EBP1 detected in m^7GTP pulldowns in p53−/− HCT116 cells (Fig. 1C), an index of unphosphorylated 4EBP1 capable of binding to capped mRNA (12); the level of elF4E adsorbed onto these beads was identical in p53+/+ and −/− cells. The diminution of the unphosphorylated form of 4EBP1 was also observed as lower levels of the fastest migrating band* detected in immunoblots of lysates from p53−/− HCT116 compared with wt p53 HCT116. These data suggest that the basal level of p53 in HCT116 cells has a substantial suppressive effect on mTORC1 activity that did not involve AMPK, and that deletion of p53 releases mTORC1 from this control.

To determine whether this effect of endogenous p53 on mTORC1 was peculiar to HCT116 or was more general, we studied mTORC1 signaling in other p53 competent carcinoma cell lines after transfection of p53 siRNA pools. In the non-small cell lung cancer (NSCLC) lines H460 and A549 as well as in HCT116 (Fig. 1D), endogenous wt p53 levels were largely eliminated by siRNA treatment; concomitantly, p-T389 S6K1 was enhanced and the level of unphosphorylated 4EBP1 was reduced, indicating a higher mTORC1 kinase activity upon

*Others have shown that 4EBP1 is phosphorylated at as many as four residues by mTORC1 and that electrophoresis in high percentage acrylamide gels can resolve several 4EBP1 species (25,30–32). The lowest band (Fig 1C, D) represents unphosphorylated 4EBP1 and the higher bands (α, β, and γ) represent species with progressively higher phosphorylation states; the phosphorylated forms are shunted to the proteasome and degraded (32).

loss of p53. We concluded that the endogenous basal level of p53 in several carcinoma cell lines was exerting a marked controlling effect on mTORC1 and that loss of endogenous p53 substantially enhanced mTORC1 kinase activity.

Mutation of p53 also causes hyperactivity of mTORC1

Human tumors lose p53 function most commonly due to mutation in one allele followed by loss of the other from the genome. Hence, we tested whether hyperactivity of mTORC1 was observed in carcinoma cells with a single allele of mutant p53 in the same genetic background. For this, p53−/− HCT116 colon carcinoma cells were stably transfected with three mutant p53 species commonly seen in clinical samples, namely R175H, R248W, and R273H. These same mutant p53 species and also V143A were stably transfected into H1299 small cell lung carcinoma cells and were compared with H1299 cells bearing a ponasterone-A-inducible p53 gene. Ponasterone-A induced wt p53 in H1299 reduces mTORC1 activity as seen by the decreased phosphorylation of S6K1 and 4EBP1, and increased levels of unphosphorylated 4EBP1 (Fig. 2B). In both HCT116 and H1299 cells (Fig 2A,B), mTORC1 targets, S6K1 and 4EBP1, were as hyperphosphorylated in cells bearing any of these p53 mutant forms as they were in p53 null cells. Likewise, the binding of 4EBP1 to m^7GTP beads in lysates of the mutant p53-bearing carcinoma cells was minimal and comparably decreased from that seen in p53 wt cells as that in p53-null cells (Fig. 2 C,D). We concluded that these mutant p53 proteins could not reinstate the control of mTORC1: despite the high levels of p53 expression typical of p53 mutant tumors, hyperactivity of mTORC1 was equivalent to that in p53 null cells. Hence, one of the functions of basal levels of wild-type p53 is to exert a control on mTORC1 that is missing in the mutants.

Immunoprecipitation of the mTORC1 complex shows enhanced kinase activity in cells lacking p53

In vitro kinase assays on mTORC1 complexes immunoprecipitated with an antibody against Raptor indicated higher mTORC1 kinase activity in p53−/− HCT116 cells than in p53+/+ cells (Fig 3A,B). Hence, the differences responsible for the enhanced kinase activity of mTORC1 from p53 null cells in either the components of this complex or the post-translational modifications of these components were at least partially stable to immunoprecipitation. The composition of the isolated IPs was investigated. The level of Raptor and AMPK-dependent phosphorylation of Raptor at S792 were equivalent in IPs from p53 wt and null cells (Fig 3C, left panels). Although the level of mTOR seen in lysates was unchanged (Fig 3C, right panels), the amount of total mTOR associated with Raptor was enhanced in p53 deficient cells (Fig 3C, left panels, and 3D), apparently reflecting a redistribution of cellular mTOR into mTORC1 complexes. mTOR bound to Raptor IPs increased by 63 ± 5 % (3 experiments) in p53 null HCT116 cells. The Raptor-bound mTOR had higher p-S2448, a modification catalyzed by S6K1, but this appears to reflect the higher levels of mTOR bound to Raptor (Fig 3C-left panels). Although the levels of PRAS40 and of p-T246 PRAS40 were unchanged in lysates of p53 null cells, the binding of total and p-T246 PRAS40 to anti-Raptor IPs was lower in p53 null cells (Fig. 3C-left panels and 3D). Contrary to the levels of the other components, the levels of TSC2 were decreased in lysates of p53-null cells (Fig 3C-right panel and Fig 6A), as they also were in lysates of all of the mutant p53s studied (Fig 6A). Apparently as a result of these lower expression levels of

TSC2, the level of TSC2 in the IPs from p53 null cells was decreased compared to that in p53 wt cells (Fig 3C-left panels, and 3D). Overall, there were higher levels of mTOR in mTORC1 complexes in p53 null HCT116 cells and a lower content of PRAS40 and TSC2 bound to mTORC1, factors that would promote higher mTORC1 kinase activity (14, 26).

Membrane localization of components of the mTORC1 complex in p53 wild type and null carcinoma cells

Previous studies (5,6) have shown that the localization of mTORC1 components to endomembranes is intrinsic to the control of this complex and that growth factor stimulation of mTORC1 activity is associated with the release of TSC2 from membrane sites containing bound mTORC1. We applied the conditions of membrane isolation used in these precedent studies to determine whether loss of p53 affected subcellular localization of the components of mTORC1. By isolation of total membrane fractions using the conditions applied by Walker and colleagues (5), we found that mTOR was largely in membrane fractions as was Raptor, and the membrane localization of these components was not affected by p53 loss (Fig 4A). PRAS40, the inhibitor of mTORC1, was distributed between the membrane fraction and the cytosol and was not measurably affected by p53 status. However, there was a marked decrease in total TSC2, as well as in membrane bound TSC2 levels in p53−/− cells (Fig 4A) that was in agreement with the results of the Raptor IP studies (Fig 3C), apparently a result of the lower total expression of TSC2 (see below). Concurrently, more Rheb was detected in the membrane fraction of p53−/− cells than in isogenic p53 wt HCT116 (Fig. 4A). We next applied the separation conditions described by Menon et al (6) that allowed the fractionation of heavy membranes containing lysosomal components from a fraction containing light membranes and cytosolic components. The loss of p53 resulted in a lower level of TSC2 in heavy membranes marked by the presence of the lysosomal protein LAMP1 (Fig. 4B). Rheb levels again showed the opposite pattern, with more detectable in the heavy membrane in p53 null cells than in wt cells (Fig. 4C). We concluded that loss of p53 function resulted in a loss of TSC2 from the membrane bound sites where mTORC1 activity was concentrated and that, with lower TSC2 levels, a higher content of the mTORC1 activator Rheb was detectable in heavy membrane fractions.

We tested this conclusion by comparing TSC2 and Rheb levels in wt MEFs and MEFs that lack TSC2. While these TSC2 knockout MEFs are also p53 null, they represent a more extreme depletion of TSC2 than would be the case in HCT116 p53 null cells. These TSC2 knockout MEFs were found to have a more marked enrichment of Rheb in the membrane fraction compared to wt MEFs (Fig 4D).

p53 loss affects the localization of TSC2 and Rheb in the lysosomal compartment

Confocal microscopy was used to compare the colocalization of TSC2 and of Rheb with the lysosomal marker proteins LAMP1 and LAMP2 using previously validated (6) antibodies. TSC2 in p53 wt HCT116 cells grown in serum-containing medium was distinctly concentrated at the lysosomal membrane, as judged by colocalization with LAMP2 (Fig 5A), with some diffuse staining in the cytosol, in accord with the results from membrane fractionation studies (Fig 4). The lysosomal localization of TSC2 was much lower in p53 null cells (Fig. 5A). The converse was seen for Rheb, with higher localization in lysosomal

areas in p53−/− cells than in their wt counterparts (Fig 5B); a much higher cytosolic staining was seen with Rheb than with TSC2, again in accord with the data of Fig. 4C. The positions of staining were analyzed for 50–100 cells of each arm and colocalization of LAMP2 and TSC2 on the one hand, and LAMP1 and Rheb on the other, were calculated using Manders' colocalization coefficient (28). The results clearly showed a significant difference between wt and p53 null cells for each comparison, with less TSC2 and more Rheb localized with the lysosomal marker in p53 null cells. Since cells were maintained in full serum and medium, mTOR and Raptor are highly concentrated at lysosomal membranes, and this co-localization with LAMP2 is not changed by loss of p53 (Fig. 4 and Fig 5D). Very interestingly, the intensity of lysosomal mTOR fluorescence was not different between p53 wt and null HCT116 cells (P=0.25), so that neither the lysosomal location of mTOR nor the amount of mTOR on these membranes were appreciably different.

The enhanced Rheb levels at lysosomal membranes induced us to examine the level of Rheb in Raptor IPs. Previous studies by others (26) have demonstrated that the composition of such IPs was influenced by the salt concentration used to wash the pellets. Using the salt washes previously described for analysis of Raptor IPs for the detection of PRAS40 (150 mM) (26), the presence of Rheb in Raptor IPs was inconsistent. However, when the salt concentration of Raptor IP washes was decreased to 100 mM (Fig S1), the presence of Rheb in these IPs was apparent in p53 null HCT116 cells but not in p53 wt cells (Fig. 5F). This immunoreactivity was not seen in IgG IPs, nor was it seen in IPs immunoblotted in the presence of the peptide used to raise the human Rheb antibody (Fig 5F). We concluded that Rheb was present in mTORC1 complexes at a higher level in p53 null cells, but that it was easily removed from these complexes by salt washes. This agrees with the higher levels of Rheb detected by confocal microscopy at the lysosomal membrane in p53 null cells compared to p53 wt cells (Fig 5B).

The effect of p53 loss on TSC2 and Rheb localization at the lysosome was studied in A549 and H460 lung carcinoma cells to determine whether the effects seen in HCT116 cells could be generalized. In both H460 and A549 cells, depletion of p53 by siRNA (Fig. 1D) caused a substantial decrease of TSC2 at the lysosome and a concomitant increase in lysosomal Rheb (Fig. 5E), consistent with the increased mTORC1 activity seen in these cell lines with p53 siRNA treatment (Fig. 1D). This reciprocal relationship between binding of TSC2 at the lysosome and the levels of Rheb at this location suggests that higher TSC2 at the lysosome downregulates lysosomal Rheb.

Complementation of the control of the mTORC1 pathway in p53 null cells by exogenous expression of TSC2 and Sestrin2

The lower levels of TSC2 colocalizing with the membrane-bound mTORC1 complexes in p53 null cells led us to question the cellular levels of TSC2 and of Sestrin2, a protein involved in TSC2 function (15). The levels of both TSC2 and Sestrin2 proteins were decreased in HCT116 cells without p53 (Fig. 6A). When the steady-state levels of TSC2 and Sestrin2 mRNA were determined by RT-qPCR, both mRNA populations were diminished with loss or mutation of p53 (Fig 6B). Mutant p53, in both the HCT116 and H1299 backgrounds, led to a similar decrease in TSC2 as seen in p53 null cells (Fig 6A). The effect

of deletion of p53 on levels of TSC2 mRNA has been previously reported (18) as has the fact that DNA-damaging drugs increased Sestrin2 mRNA (19,20). Rheb mRNA levels are not affected by loss of p53 (Fig S2).

Because of the centrality of TSC2 to the control of mTORC1 kinase activity and the role of Sestrins in the localization of mTOR to the lysosome induced by amino acids (7,16,17), we questioned whether the hyperactivity of mTORC1 seen in p53−/− HCT116 cells was due to the lower levels of TSC2 and Sestrin2. When TSC2 was depleted by siRNA knockdown in HCT116 cells with wt p53 function, a dramatic increase in cellular mTORC1 activity was observed (Fig. 6C), as would be expected from the constitutive activity of mTORC1 in Tuberous sclerosis (33). Likewise, the level of mTORC1 activity was much higher in Sestrin2 −/− MEFs, compared to MEFs with wt Sestrin2 function (Fig 6D). Hence, the deficiencies of TSC2 and Sestrin2 appeared to be involved in the enhanced mTORC1 activity in p53 null/mutant cells.

To test whether exogenous replacement of TSC2 and/or Sestrin2 could prevent the hyperactivity of mTORC1 in p53 null cells, FLAG-tagged Sestrin2 or HA-TSC2 were transfected into p53−/− HCT116. The phosphorylation of S6K1 was reduced almost to the levels seen in wt HCT116 by either construct (Fig. 7A); when both constructs were cotransfected, the level of p-T389 S6K1 was identical to that in wt HCT116. Likewise, transfection of TSC2 or Sestrin2 or of both constructs into p53−/− HCT116 returned the level of 4EBP1 seen in m^7GTP pulldowns back to that seen in p53+/+ HCT116 (Fig. 7B). Hence, the hyperactivity of mTORC1 in cell lines with wild type p53 and genetically diminished TSC2 or Sestrin2 (Fig 6C,D), combined with the diminished mTORC1 activity in p53 null cells after forced expression of TSC2 or Sestrin2 (Fig. 7A,B) supports the proposed mechanism that the enhanced mTORC1 seen in p53 null cells is mediated by loss of TSC2 and Sestrin2 expression.

The mechanism whereby the forced expression of TSC2 or of Sestrin2 reverted the level of mTORC1 activity in p53 null HCT116 cells back to the level seen in wt p53 was examined by confocal microscopy. It was apparent that the higher levels of TSC2 after forced expression (Fig S3A) caused a significantly enhanced distribution of TSC2 to the lysosomal membranes with a concomitant decreased lysosomal Rheb (Fig. 7C), whereas forced expression of Sestrin2 (Fig S3B) inhibited the distribution of mTOR to the lysosome (Fig. 7D) in accord with previous studies (7,16,17) while not affecting the distribution of TSC2 to lysosomal membranes (Fig S3C)).

Overall, we concluded that a substantially enhanced mTORC1 activity is seen in p53-null or -mutant cells, coincident with lower levels of TSC2 and Sestrin2. The lower levels of TSC2 expression shifted TSC2 away from sites of mTORC1 at lysosomal membranes (Fig. 5B,D) while lower Sestrin2 did not result in lower lysosomal mTOR, although it could be involved with the higher levels of mTOR in mTORC1 complexes seen in IPs (Fig. 3). When the levels of TSC2 on lysosomes were diminished, lysosomal Rheb increased, apparently resulting in the direct stimulation of mTORC1 activity.

Discussion

The single most frequent genetic change in human tumors is mutation of the p53 gene at positions that alter the transcriptional activity of the protein. Typically, mutation in one allele is followed by a loss of the other allele, with major changes in levels of transcriptional targets of the wt protein. As a less frequent event, some tumors lose both alleles of this gene. We show here that loss of p53 upregulates mTORC1 activity. The enhancement of mTORC1 we observed in p53 null cells was also seen in carcinoma cells expressing mutant p53s even at the very high levels of this protein usually found for such mutations, a fact that emphasizes the centrality of the p53-driven transcriptional program in control of mTORC1 activity. The effect isolated by our studies is an activity mediated by the low basal steady state levels of wt p53; loss of this expression has clear effects on mTORC1 control.

We used immunoprecipitations, membrane fractionations and confocal microscopy to study how p53 alters the components of mTORC1. All three approaches indicated a shift of TSC2 away from the mTORC1 complexes, which were located at the lysosomal membrane. In concert with the decreased association of TSC2 with the position of mTORC1, there was an enhanced Rheb colocalization with mTORC1 as indicated by membrane fractionations, confocal microscopy and IPs. A decrease in PRAS40 was detectable in Raptor IPs, as was a higher distribution of mTOR into Raptor complexes. Interestingly, increased distribution of mTOR into a lysosomal membrane compartment was not seen in p53 null cells by either membrane distribution studies or confocal microscopy.

When the transcriptional activity of p53 is lost from carcinoma cells, the levels of TSC2 and Sestrin2, two p53 targets known to impact control of mTORC1, fall. We have studied the role of diminished levels of TSC2 and of Sestrin2 in the enhanced mTORC1 activity seen in p53 null or mutant cells. Genetic deficiency of either TSC2 or Sestrin2 results in enhanced mTORC1 activity (Fig 6C,D). The critical intermediate step that mediates this increase in mTORC1 activity appears to be the lower expression of TSC2. The current literature suggests that redistribution of TSC2 to lysosomal membranes plays an intrinsic role in control of mTORC1 activity in response to insulin (6). When p53 transcriptional activity is lost, TSC2 levels are lower and the partitioning of TSC2 to the lysosome is decreased; enforced expression of TSC2 in p53 null cells reinstates TSC2 levels and TSC2 partitioning to the lysosome. These shifts in TSC2 off and back onto the lysosome argue for causality of TSC2 in the enhanced mTORC1 activity. The shifts of TSC2 off lysosomal membranes in p53 null cells and back on when TSC2 expression was forced was, surprisingly, associated with opposing and distinct changes in lysosomal Rheb at or near bound mTOR and Raptor. This effect was more obvious using the least disruptive technique we applied, confocal microscopy (Fig 5B), as well as by membrane fractionations of cells completely lacking TSC2 expression, i.e., TSC2-null MEFs (Fig 4D).

The role of decreased Sestrin2 levels in p53 null cells on mTORC1 activity was more difficult to determine. Three recent papers (7,16,17) indicate the involvement of the Sestrins in mTOR localization at lysosomal membranes in response to amino acids. The effects of Sestrin2 on mTOR distribution are clearly dependent on level of expression: Sestrin2 levels created by forced expression (Fig S3B), substantially decreased mTOR levels on lysosomes

(Fig 7D), but the decrease in Sestrin2 in p53 null cells did not cause a shift of mTOR onto the lysosomal membranes. We could not determine whether it might explain the increased association of mTOR with lysosomal Raptor which contributed to the increased mTORC1 activity in p53 null cells. Whether the level of Sestrin2 following DNA damage stabilization of p53 would affect mTOR distribution to the lysosome also remains to be seen.

This proposed model to explain our results, summarized in Fig. 7E, reflects the current view of a dynamic equilibrium in the binding of TSC2 at the lysosomal membrane and of Sestrin2 on mTOR partitioning, both affecting mTORC1 activity, but further suggests that the role of TSC2 involves exclusion of Rheb at the lysosome.

Supplementary Material

Refer to Web version on PubMed Central for supplementary material.

Acknowledgments

This work was supported by grant R01-CA140416 from the NIH. We thank Drs Bert Vogelstein, Jennifer Pietenpol, and Andrei Budanov for valuable cell lines and Dr Andrei Budanov for helpful discussions. We thank Dr. Scott Henderson for his insightful and valuable assistance on confocal microscopy. Microscopy was performed at the VCU Department of Anatomy and Neurobiology Microscopy Facility, supported in part by a NIH-NINDS Center Core grant (5P30NS047463); additional assistance was obtained by the Massey Cancer Center Macromolecule Core Facility under NIH grant P30-CA016059.

References

1. Kim SG, Buel GR, Blenis J. Nutrient regulation of the mTOR complex 1 signaling pathway. Mol Cells. 2013; 35:463–73. [PubMed: 23694989]
2. Sabatini DM. mTOR and cancer: insights into a complex relationship. Nat Rev Cancer. 2006; 6:729–34. [PubMed: 16915295]
3. Hay N, Sonenberg N. Upstream and downstream of mTOR. Genes Dev. 2004; 18:1926–45. [PubMed: 15314020]
4. Schalm SS, Fingar DC, Sabatini DM, Blenis J. TOS motif-mediated raptor binding regulates 4E-BP1 multisite phosphorylation and function. Curr Biol. 2003; 13:797–806. [PubMed: 12747827]
5. Cai SL, Tee AR, Short JD, Bergeron JM, Kim J, Shen J, et al. Activity of TSC2 is inhibitedby AKT-mediated phosphorylation and membrane partitioning. J Cell Biol. 2006; 173:279–89. [PubMed: 16636147]
6. Menon S, Dibble CC, Talbott G, Hoxhaj G, Valvezan AJ, Takahashi H, et al. Spatial control of the TSC complex integrates insulin and nutrient regulation of mTORC1 at the lysosome. Cell. 2014; 156:771–85. [PubMed: 24529379]
7. Chantranupong L, Wolfson RL, Orozco JM, Saxton RA, Scaria SM, Bar-Peled L, et al. The Sestrins interact with GATOR2 to negatively regulate the amino-acid-sensing pathway upstream of mTORC1. Cell Rep. 2014 Oct 9; 9(1):1–8. [PubMed: 25263562]
8. Sancak Y, Peterson TR, Shaul YD, Lindquist RA, Thoreen CC, Bar-Peled L, et al. The Rag GTPases bind raptor and mediate amino acid signaling to mTORC1. Science. 2008 Jun 13; 320(5882):1496–501. [PubMed: 18497260]
9. Sancak Y, Bar-Peled L, Zoncu R, Markhard AL, Nada S, Sabatini DM. Ragulator-Rag complex targets mTORC1 to the lysosomal surface and is necessary for its activation by amino acids. Cell. 2010; 141(2):290–303. [PubMed: 20381137]
10. Bar-Peled L, Schweitzer LD, Zoncu R, Sabatini DM. Ragulator is a GEF for the rag GTPases that signal amino acid levels to mTORC1. Cell. 2012 Sep 14; 150(6):1196–208. [PubMed: 22980980]

11. Bar-Peled L, Chantranupong L, Cherniack AD, Chen WW, Ottina KA, Grabiner BC, et al. A Tumor suppressor complex with GAP activity for the Rag GTPases that signal amino acid sufficiency to mTORC1. Science. 2013 May 31.340(6136)
12. Garami A, Zwartkruis FJ, Nobukuni T, Joaquin M, Roccio M, Stocker H, et al. Insulin activation of Rheb, a mediator of mTOR/S6K/4E-BP signaling, is inhibited by TSC1 and 2. Mol Cell. 2003; 11:1457–66. [PubMed: 12820960]
13. Sato T, Nakashima A, Guo L, Tamanoi F. Specific activation of mTORC1 by rheb G-protein in vitro involves enhanced recruitment of its substrate protein. J Biol Chem. 2009; 284:12783–91. [PubMed: 19299511]
14. Tee AR, Manning BD, Roux PP, Cantley LC, Blenis J. Tuberous sclerosis complex gene products, Tuberin and Hamartin, control mTOR signaling by acting as a GTPase-activating protein complex towards Rheb. Curr Biol. 2003; 13:1259–68. [PubMed: 12906785]
15. Budanov AV, Karin M. p53 target genes Sestrin1 and Sestrin2 connect genotoxic stress and mTOR signaling. Cell. 2008; 134:451–60. [PubMed: 18692468]
16. Parmigiani, Anita; Nourbakhsh, Aida; Ding, Boxiao; Wang, Wei; Kim, Young Chul; Akopiants, K., et al. Sestrins Inhibit mTORC1 Kinase Activation through the GATOR. Complex Cell Reports. 2014; 9:1281–1291. [PubMed: 25457612]
17. Peng, Min; Yin, Na; Li, Ming O. Sestrins function as guanine nucleotide dissociation inhibitors for Rag GTPases to control mTORC1 signaling. Cell. 2014; 159:122–133. [PubMed: 25259925]
18. Feng Z, Hu W, de Stanchina E, Teresky AK, Jin S, Lowe S, et al. The regulation of AMPK β1, TSC2, and PTEN expression by p53: Stress, cell and tissue specificity, and the role of these gene products in modulating the IGF-1-AKT-mTOR pathways. Cancer Research. 2007; 67:3043–53. [PubMed: 17409411]
19. Budanov AV, Shoshani T, Faerman A, Zelin E, Kamer I, Kalinski H, et al. Identification of a novel stress-responsive gene Hi95 involved regulation of cell viability. Oncogene. 2002; 21:6017–31. [PubMed: 12203114]
20. Velasco-Miguel S, Buckbinder L, Jean P, Gelbert L, Talbott R, Laidlaw J, et al. PA26, a novel target of the p53 tumor suppressor and member of the GADD family of DNA damage and growth arrest inducible gene. Oncogene. 1999 Jan 7; 18(1):127–37. [PubMed: 9926927]
21. Feng Z, Zhang H, Levine AJ, Jin S. The coordinate regulation of the p53 and mTOR pathways in cells. Proc Natl Acad Sci USA. 2005; 102:04–8209.
22. Flatt PM, Tang LJ, Scatena CD, Szak ST, Pietenpol JA. p53 regulation of G(2) checkpoint is retinoblastoma protein dependent. Mol Cell Biol. 2000; 20(12):4210–23. [PubMed: 10825186]
23. Racanelli AC, Rothbart SB, Heyer CL, Moran RG. Therapeutics by cytotoxic metabolite accumulation: pemetrexed causes ZMP accumulation, AMPK activation, and mammalian target of rapamycin inhibition. Cancer Res. 2009; 69:5467–5474. [PubMed: 19549896]
24. Rothbart SB, Racanelli AC, Moran RG. Pemetrexed indirectly activates the metabolic kinase AMPK in human carcinomas. Cancer Res. 2010; 70:10299–10309. [PubMed: 21159649]
25. Holz MK, Ballif BA, Gygi SP, Blenis J. mTOR and S6K1 mediate assembly of the translation preinitiation complex through dynamic protein interchange and ordered phosphorylation events. Cell. 2005; 123:569–80. [PubMed: 16286006]
26. Sancak Y, Thoreen CC, Peterson TR, Lindquist RA, Kang SA, Spooner E, et al. PRAS40 is an insulin-regulated inhibitor of the mTORC1 protein kinase. Mol Cell. 2007; 25:903–915. [PubMed: 17386266]
27. Bronder JL, Moran RG. A defect in the p53 response pathway induced by de novo purine synthesis inhibition. J Biol Chem. 2003; 278:48861–71. [PubMed: 14517211]
28. Manders EM, Stap J, Brakenhoff GJ, van Driel R, Aten JA. Dynamics of three-dimensional replication patterns during the S-phase, analyzed by double labelling of DNA and confocal microscopy. J Cell Sci. 1991; 103:857–86. [PubMed: 1478975]
29. Inoki K, Li Y, Zhu T, Wu J, Guan KL. TSC2 is phosphorylated and inhibited by Akt and suppresses mTOR signalling. Nat Cell Biol. 2002; 4(9):648–57. [PubMed: 12172553]
30. Herbert TP, Tee AR, Proud CG. The extracellular signal-regulated kinase pathway regulates the phosphorylation of 4E-BP1 at multiple sites. J Biol Chem. 2002; 277:11591–6. [PubMed: 11799119]

31. Gingras AC, Raught B, Sonenberg N. Regulation of translational initiation by FRAP/mTOR. Genes Dev. 2001; 15:807–26. [PubMed: 11297505]

32. Ma XM, Blenis J. Molecular mechanisms of mTOR-mediated translational control. Nat Rev Mol Cell Biol. 2009; 10:307–318. [PubMed: 19339977]

33. Kwiatkowski DJ, Manning BD. Tuberous sclerosis: a GAP at the crossroads of multiple signaling pathways. Human Mol Genet. 2005; 14:R251–8. [PubMed: 16244323]

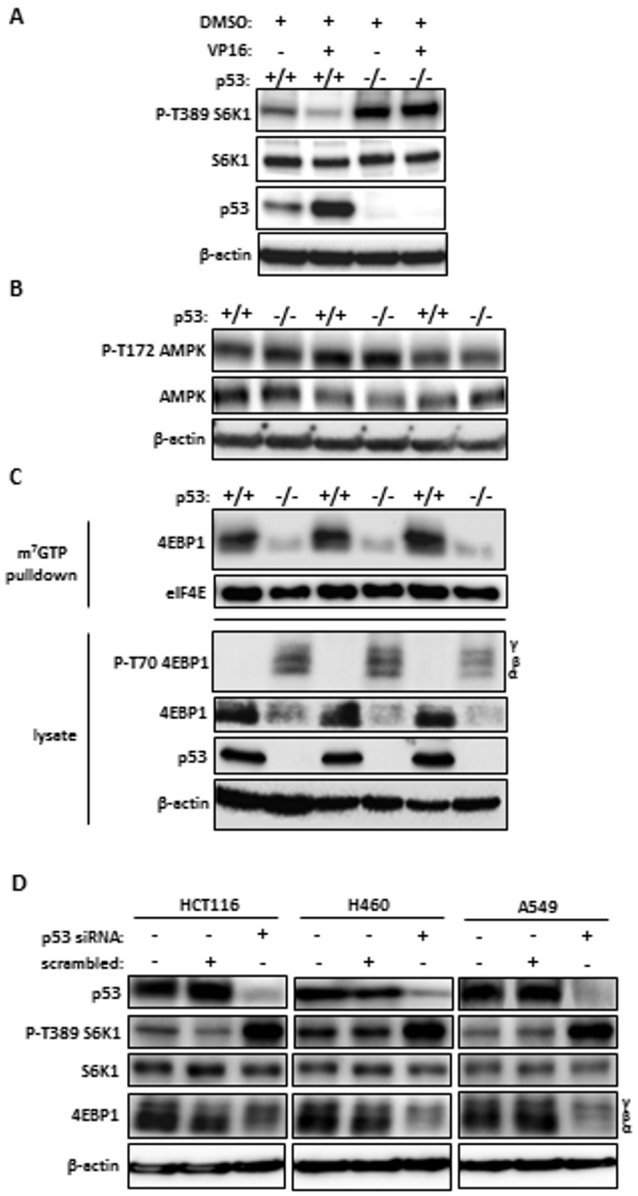

Figure 1. mTORC1 activity is enhanced with loss of p53 function independent of AMPK

(A) *Phosphorylation of S6K1 is higher in p53 null cells.* p53+/+ and p53−/− HCT116 cells were treated with vehicle (DMSO) or 20 μM VP16 for 24 hrs and p53 and p-T389 S6K1 levels were assessed by immunoblotting. (B) *Loss of p53 does not alter activation of AMPK*. Three subconfluent cultures of HCT116 cells wt and null for p53 were separately harvested and lysates probed by immunoblotting. (C) *p53 null cells have higher mTORC1-dependent phosphorylation of 4EBP1 and reduced 4EBP1 function.* m^7GTP pulldowns were performed on 3 independent replicate HCT116 cell lysates followed by immunoblot analysis of the eIF4E and 4EBP1 captured by the beads, as well as the corresponding lysates. (D) *Silencing of p53 augments mTORC1 signaling.* HCT116 and two NSCLC cell lines, H460 and A549, were transfected with scrambled or p53-specific siRNA for 48 hrs and cell extracts were analyzed by immunoblotting.

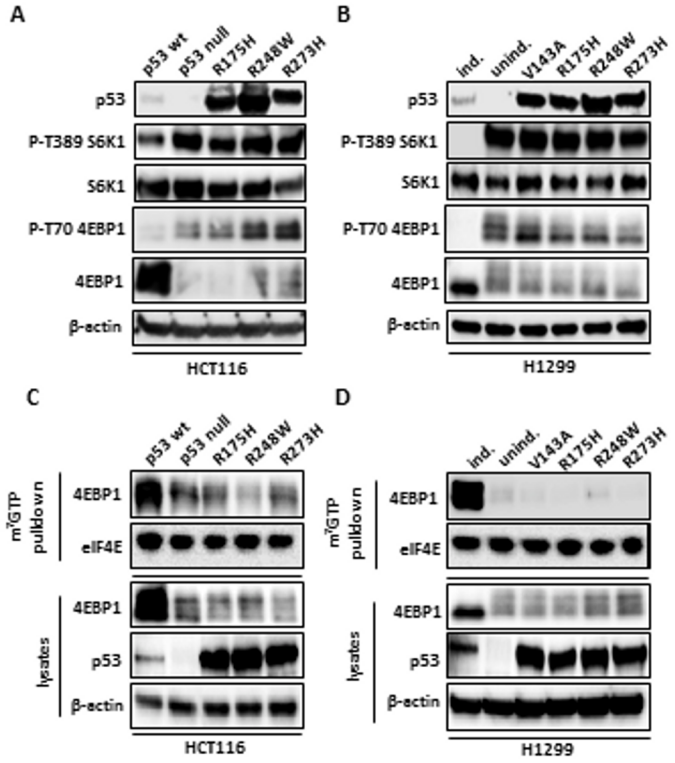

Figure 2. Mutations in the DNA binding domain of p53 enhance mTORC1 activity equivalently to loss of p53

The expression and phosphorylation of S6K1 and 4EBP1 were determined by immunoblotting of HCT116 p53−/− cells stably transfected with hot spot mutants of p53 (A) or in similarly transfected H1299 cells (B) and compared with HCT116 and their isogenic p53−/− cells or H1299 transfected with an inducible p53 construct, respectively. The binding of 4EBP1 to m^7GTP bound beads is severely depressed in HCT116 (C) or H1299 cells stably transfected with p53 mutants (D). In (B and D) ind. and unind. refer to induced and uninduced.

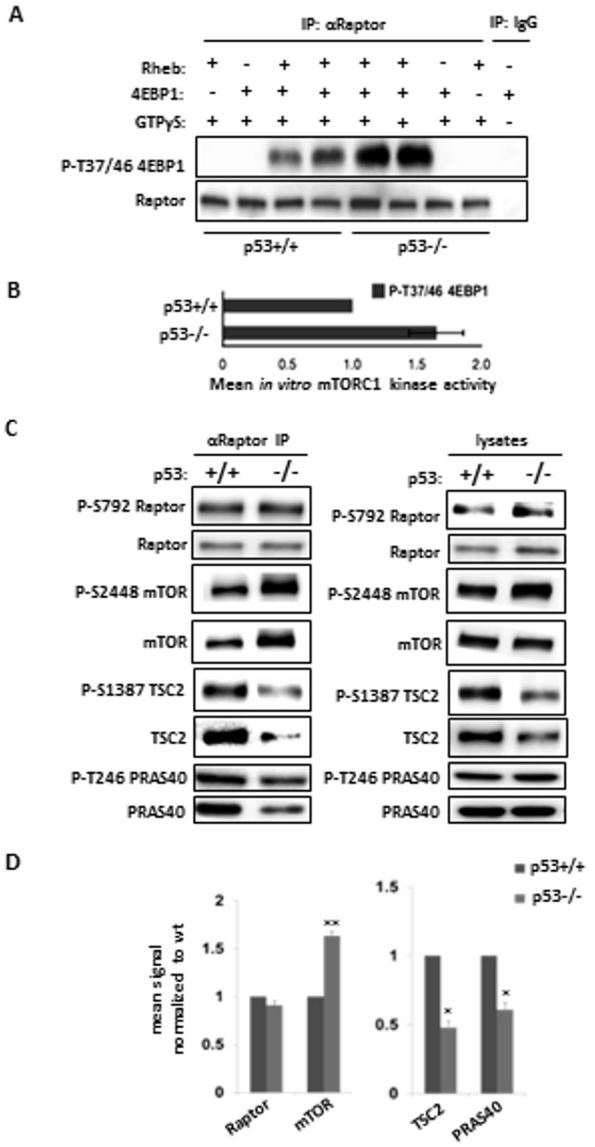

Figure 3. The enhanced kinase activity of the mTORC1 complex is retained during immunoprecipitation in cells lacking p53

(A) The mTORC1 complex from p53−/− cells has enhanced kinase activity in vitro. mTORC1 was immunoprecipitated with an anti-Raptor antibody under low salt (100 mM) conditions and *in vitro* kinase assays were performed using 4EBP1 as a substrate; p-T37/46 4EBP1 generated was determined by immunoblot. (B) Licor densitometry data from 3 independent *in vitro* kinase assays (mean ±sd). (C) *The components of the mTORC1 complex differ between p53+/+ and p53−/− cells.* Anti-Raptor immunoprecipitates (IPs) from isogenic HCT116 cells were probed with antibodies against the indicated proteins; lysates were probed in parallel. Equivalent IPs using IgG that were processed and exposed equally were uniformly blank (not shown). (D) The level of Raptor, mTOR, PRAS40, and TSC2 in p53-null HCT116 cells was measured by densitometry from 3 independent experiments and

expressed (±sd) relative to the level in p53 wt control cultures.**p=0.0045 for mTOR, *p=0.048 for TSC2, *p=0.0117 for PRAS40.

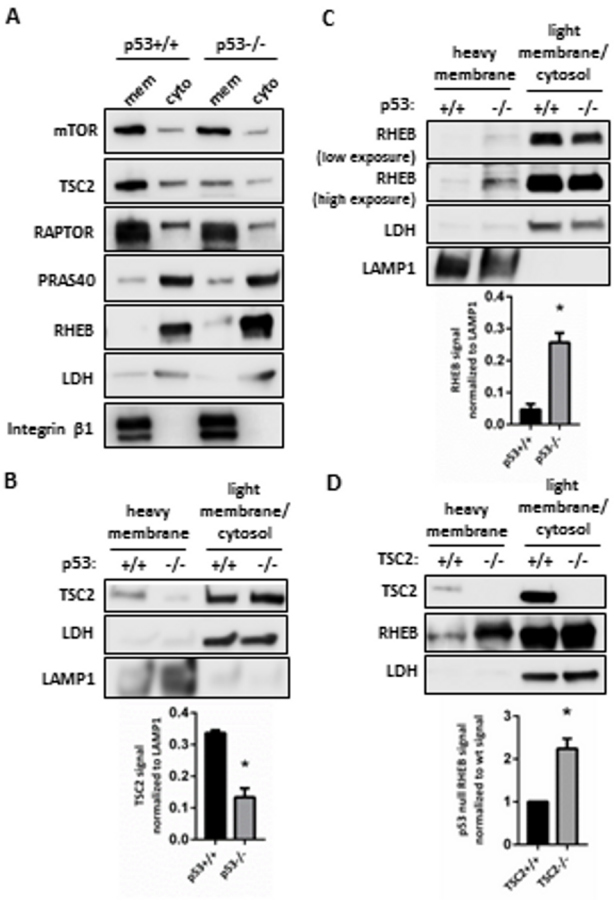

Figure 4. Distribution of components of the mTORC1 complex in endomembranes and cytosol

Membranes were separated from cytosol as in (5) in HCT116 cells (A) or were fractionated as in (6) for isolation of heavy membranes containing lysosomal membrane (B, C, D) from light membranes and cytosol, and immunoblotted for components of the mTORC1 complex. (D) Fractionated membranes from MEFs wt or null for TSC2. TSC2 −/− MEFs can only be made in a p53 −/− background. LDH was used as a cytosolic marker, Integrin β1 for membranes, and LAMP1 for lysosomal membranes (The LAMP1 antibody does not detect the mouse epitope in D). The bar graphs represent data from 3 experiments (mean ± SEM). TSC2 in heavy membrane fractions was significantly lower in p53 null cells ((B) * denotes p= 0.004) and Rheb was significantly higher compared to p53 wt HCT116 ((C) p= 0.002). There were significantly higher Rheb levels in heavy membranes from TSC2 null MEFs ((D) p= 0.007).

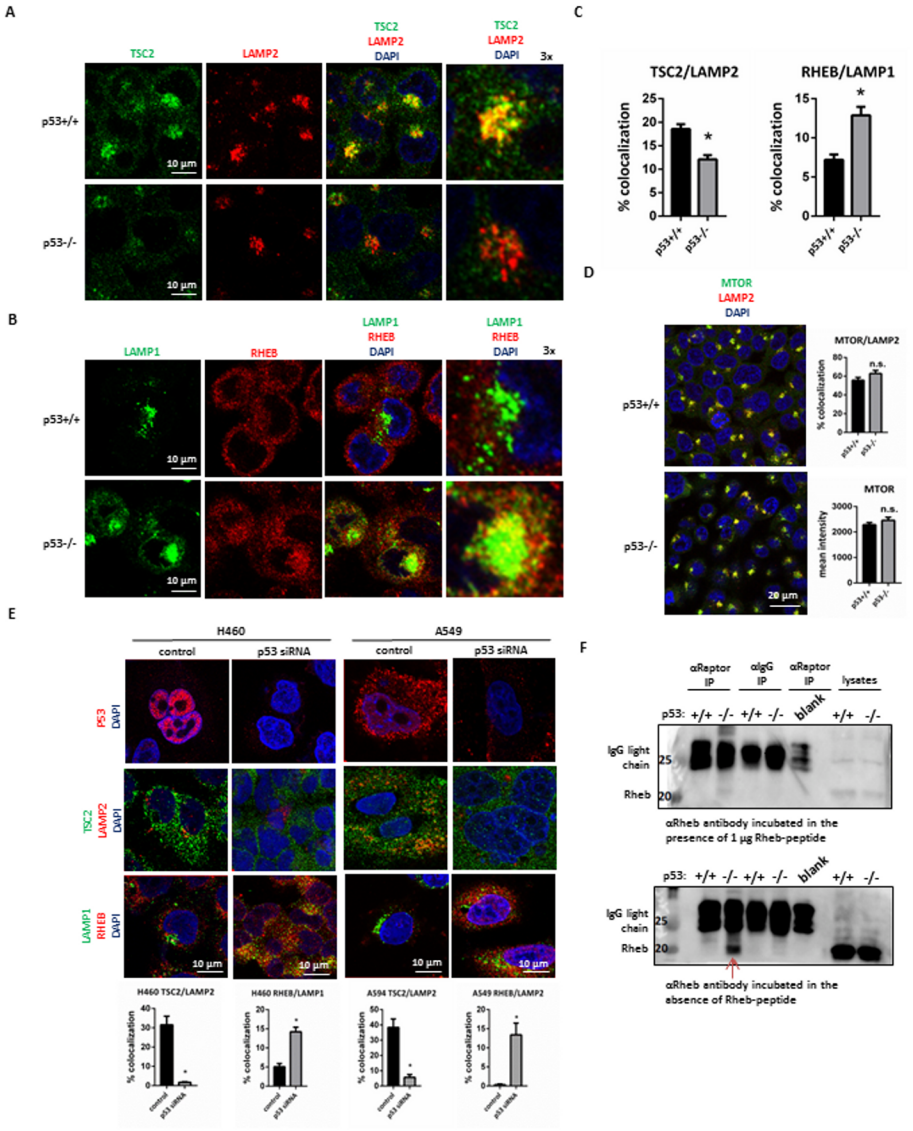

Figure 5. Loss of p53 decreases the distribution of TSC2 to and increases the level of Rheb in lysosomal membranes

(A) *Confocal microscopy of the colocalization of endogenous TSC2 and the lysosomal marker LAMP2.* Endogenous TSC2 (green) and LAMP2 (red) were subjected to immunofluorescence labeling in wt and p53 null HCT116 cells. (B) Endogenous LAMP1 (green) and Rheb (red) were imaged in HCT116 cells as in (A). (C) Bar graphs show Manders' colocalization coefficient for >50 cells expressed as a percentage ±SEM; the differences between wt and p53 null cells are significant for both comparisons (*p = 0.0001). (D) *mTOR colocalized with LAMP2 in HCT116 cell wt or null for p53*. Neither the degree of colocalization, nor the intensity of lysosomal mTOR differed between HCT cells with or without p53. (E) *siRNA knockdown of p53 in H460 and A549 cells recapitulates the changes in lysosomal TSC2 and Rheb seen in HCT116 cells.* TSC2 and Rheb colocalization with lysosomal markers LAMP1 and LAMP2 were quantitated as in panel C and are presented as means ± SEM (n=20). The differences between scrambled and siRNA for p53

were highly significant (P< 0.0001) for TSC2 distribution in both cell lines and for Rheb in H460 and at p=0.0004 for A549 and Rheb distribution. (F). *Detection of Rheb in Raptor IPs from p53 null cells washed with low salt.* Raptor IPs were washed with 100 mM salt prior to immunoblotting gels that were run long enough to separate IgG from Rheb. Note that the Rheb antibody cross-reacted with IgG but that a band corresponding to Rheb was found in p53 null cells but not p53 wt cell IPs that was absent in IgG IPs. Incubation of the Rheb antibody with its epitope peptide (1 μg/ml) blocked the detection of Rheb but not the IgG bands. The position of Rheb (red arrow) is marked by the location of the immunoreactive bands in lysates of HCT wt (+/+) and HCT p53 null (−/−) shown at the right. Blank indicates mixtures without lysate.

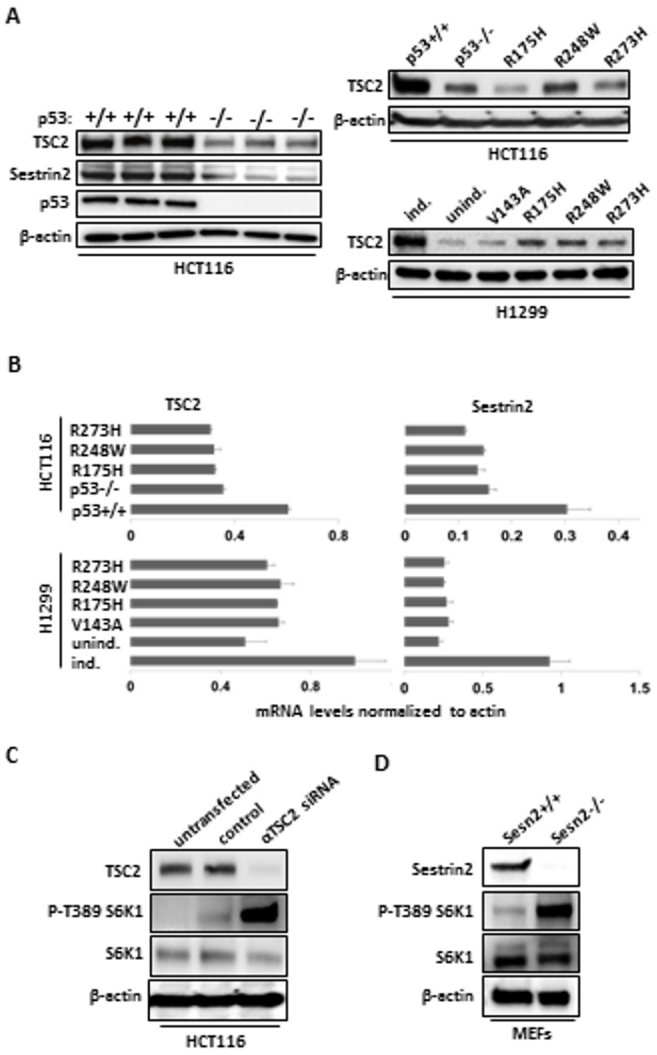

Figure 6. Levels of TSC2 and Sestrin2 mRNA and protein in carcinoma cells that are p53 null or that express only mutant p53

(A) *TSC2 protein levels determined by immunoblot of lysates.* (B) *TSC2 and Sestrin2 mRNA levels were measured by RT-qPCR using total RNA.* (mean ± sd, n=3). *siRNA depletion of TSC2 (C) or genetic deletion of Sestrin2 (D) substantially increase the level of mTORC1 activity.* HCT116 cells wt for p53 were transfected with siRNA against TSC2 or a scrambled control and mTORC1 activity was assessed by phosphorylation of S6K1 at T389 (C). MEFs from mice with genetic deletion of Sestrin2 were likewise probed for pT389-S6K1 (D).

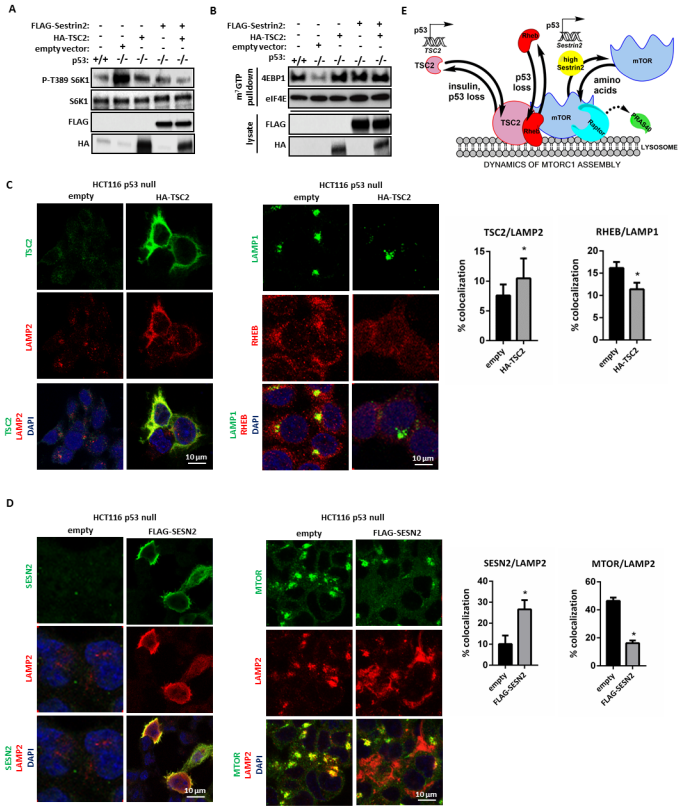

Figure 7. Forced expression of TSC2 and/or Sestrin2 decreases the elevated mTORC1 *activity in p53 null cells down to levels seen in p53 wt cells*

(A) FLAG-tagged Sestrin2, HA-TSC2, or an empty vector control were transfected into p53−/− HCT116 cells, alone or in combination, and the degree of p-T389 S6K1 was visualized by immunoblotting. *(B) Forced expression of TSC2 and/or Sestrin2 in p53 null cells increases m^{7}GTP cap binding.* m^{7}GTP pulldown assays were performed on p53−/− HCT116 cells following transfection with the constructs in (A) and levels of bound 4EBP1 and eIF4E were detected by immunoblotting. (C) *Transfection of HA-TSC2 into HCT116 cells null for p53 restores lysosomal TSC2 and diminishes Rheb at lysosomal membranes.* The increase in lysosomal TSC2 and decrease in lysosomal Rheb were statistically significant (p= 0.024 and 0.036, respectively, n = 40). (D) *Transfection of Flag-Sestrin2 into HCT116 cells null for p53 decreases partitioning of mTOR to the lysosome.* The distribution of both Sestrin2 (SESN2) and of mTOR to the lysosome was significantly different after transfection (p<0.01 (n = 40) and < 0.0001 (n = 60), respectively). TSC2 localizations to the lysosomes in these cell populations were not significantly different (Fig. S3). (E) *Proposed mechanism of p53 involvement in control of mTORC1.* In cells with basal wt p53 function, p53-dependent transcription supplies adequate levels of TSC2 and sestrin2 to regulate mTORC1 kinase activity; when cells lose p53 transcriptional activity, TSC2 and Sestrin2 levels are low, TSC2 binding at the lysosomal sites of mTORC1 is low, Rheb levels are higher at these sites, and PRAS40 is lower in mTORC1 complexes, enhancing mTORC1 activity. When Sestrin2 is high, as after transfection, the distribution of mTOR to the lysosome is dramatically decreased. When Sestrin2 is decreased from unstressed steady state levels, due to loss or mutation of p53, the distribution of mTOR onto lysosomal membranes

is unchanged. In p53 deficient cells the association of lysosomal mTOR with Raptor is increased, an effect that also increases mTORC1 activity, but it remains unclear whether Sestrin2 levels play a role in this effect.